RSC Advances

ROYAL SOCIETY OF CHEMISTRY

www.rsc.org/advances

Mechanistic insight into active chlorine species mediated electrochemical degradation of recalcitrant phenolic polymers

S. Sundarapandiyan[a], T. Shiny Renitha[b], J. Sridevi[b], B. Chandrasekaran[b], P. Saravanan[b], G. Bhaskar Raju[a*]

[a] *National Metallurgical Laboratory (Council of Scientific & Industrial Research, New Delhi), Madras centre, CSIR Complex, Taramani, Chennai 600 113, India*

[b] *Central Leather Research Institute (Council of Scientific & Industrial Research, New Delhi), Adyar, Chennai 600 020, India*

* Corresponding author, Email: gbraju55@gmail.com, sundargts@gmail.com, Phone: +91 44 22542523.

ABSTRACT

Degradation of recalcitrant phenolic syntan by electro-oxidation was investigated. The kinetics of mineralization of phenolic syntan was followed both in terms of TOC and COD measurements. The generation of oxidants such as Cl_2, HOCl and free radicals of oxychloride in the presence of NaCl electrolyte was also monitored and their role in the oxidation of organics was discussed. The generation of $^{*}ClO$ free radical was ascertained by electron spin resonance (ESR) spectroscopy coupled with spin trapping technique. The effect of pH, electrolyte concentration and current density on the degradation of phenolic syntan was discussed. Also, the current efficiency (CE) and energy consumption (EC) was estimated. It was observed that the oxidation of phenolic syntan was proportional to the current density and electrolyte concentration. The kinetics of the degradation of phenolic syntan was found to follow first order rate equation with an R^2 value of 0.9966. The intermediate compounds formed during electrooxidation were characterised using AOX, FT-IR and NMR techniques and the degradation pathway was proposed. These results clearly suggest the effectiveness of electrochemical technique for the treatment of wastewater containing high concentration of phenolic syntan.

Keywords: Phenolic syntan; electro-oxidation; degradation; ESR study; free radicals; nuclear magnetic resonance; degradation kinetics.

Introduction

The impact of leather processing on environment is considered to be very significant (Ludvik, 2000). About 30-35 m^3 of water and 700 kg of chemicals are used for converting 1 tonne of hide/skin into leather.[1] Though the pre-tanning operations contribute 70% of pollution load, the pollutants generated are simple and easy to treat. Conversely, the complex chemicals used in post-tanning process also called as wet-finishing process renders the wastewater highly complex and difficult to treat. Wide range of chemical products such as synthetic tannins (syntans), fat-liquors and dyes are used during wet-finishing processes.[2] The syntans are complex synthetic phenolic polymers synthesized using phenol as basic molecule. The unutilized / unadsorbed phenolic syntans in wastewater poses serious challenge to environment because of their poor biodegradability. The concentration of phenolic resin in tannery wastewater varies from 200 to 1500 mg/L and depends on the degree of uptake.

The phenol and phenolic products are environmentally hazardous and toxic to aquatic organisms and mankind.[3] Many techniques such as coagulation and flocculation, biological treatment, adsorption, ultrafilteration, ozonationand sonochemical degradation had been attempted for the treatment of phenolic wastewater.[4-8] The biodegradation of phenolic compounds is difficult because phenols are toxic to common microorganism. Though the advanced oxidation techniques such as photochemical degradation, ozonation and sonication are effective, the operating costs are high.[9,10] The electrochemical treatment is effective for the treatment of wastewater containing organic compounds. It has been extensively studied for the treatment of various pollutants generated from tanneries, textile industries, olive oil mills and other organic chemicals such as nonyl phenol ethoxylates, benzoquinone and chlorophenols.[11-18] Recently several attempts have been made to treat the phenol by electrochemical methods.[19-23] The electrochemical degradation of phenol using Ti/ RuO_2-Pt was studied and reported that the phenol could be completely degraded by electrooxidation.

In the present study, degradation of synthetic phenolic resin (syntan) by electro-oxidation technique using $IrO_2/RuO_2/TiO_2$ coated titanium as electrodes was reported. The generation of active chlorine especially the free radicals during electro-oxidation was examined by ESR technique and FT-IR & NMR techniques are used to identify the intermediate compounds. The oxidation kinetics of phenolic syntan and its degradation path was attempted.

Results and discussion

Effect of pH, electrolyte concentration and current density of Electro-oxidation

The effect of initial pH on the degradation of phenolic polymer was studied by varying the pH between 2.0 to 10.0. Electro-oxidation of phenolic syntan prepared in 2% NaCl solution was carried out at a constant current density of 0.015 A/cm^2. The results in terms of TOC with respect to time at different pH values are shown in Fig. 2. From the results, it is apparent that the degradation of syntan within 120 minutes of electro-oxidation was found to be hardly 45% and the effect of pH on the degradation is very marginal. Though the cell voltage remained almost constant during electrolysis, the final pH of the solution was found to shift to 7.8-8.5 irrespective of its initial value. This may be attributed to the production of CO_2 during electro-oxidation of syntan which intern dissolve in water and generates H^+ and HCO_3^-. The H^+ ions thus generated are cathodically reduced to hydrogen gas whereas HCO_3^- acts as buffering agent.

$$R + MO_x(OH)z \rightarrow CO_2 + zH^+ + ze_2 + MO_x \quad (1)$$

$$CO_2 + H_2O \rightarrow H^+ + HCO_3^- \quad (2)$$

$$2H^+ + 2e^- \rightarrow H_2\,(g) \quad (3)$$

The insitu generation of chlorine and its role in electrooxidation was investigated at different NaCl concentrations by keeping the current density and pH at 0.015 A/cm^2 and 10.0

respectively. The initial pH was kept at 10.0 as the degradation is slightly better in alkaline medium. The results presented in Fig. 2 clearly illustrate the effect of NaCl on the degradation of organics. It was observed that the TOC decreases by increasing the concentration of NaCl. However, the decrease in TOC is very marginal beyond the salt concentration of 3%. The concentration of Cl^- in the reactor was measured and found to decrease 1450 ppm within half an hour. The Cl_2 discharge from the anode in the presence of NaCl can be represented as

$$2Cl^- \rightarrow Cl_2 + 2e^- \quad (4)$$

The chlorine gas thus generated is soluble in water to form HOCl according to the following reaction. It is also known that chlorine is soluble in water to the extent of 6g/L.

$$Cl_2 + H_2O \rightarrow HOCl + H^+ + Cl^- \quad (5)$$

The change in pattern of UV-Visible spectrum of syntan solution during electrooxidation was monitored over a wavelength range of 200-800 nm. The maximum absorbance noticed around 280 nm (Fig. 3) may be attributed to n-π^* transitions of syntan molecule.[24] After 30 minutes of electro-oxidation, the peak at 280 nm was found to disappear and the colour of the wastewater turned to dark brown. The dark brown colour also ultimately disappears over a period of time. The change in colour could be attributed to various of intermediate products. The peak at 290 nm could be attributed to the presence of OCl^-. This spectrum is consistent with that of hypochlorite solution in basic medium (Fig.3, inset). Thus the generation of hypochlorite can be confirmed during electrooxidation. The shoulder around 350 nm may be due to the presence of ClO_2 formed as a result of reaction between Cl_2 and O_3 generated due to secondary electrochemical reactions. The broad peak between 275-350 nm may be interpreted due to merger of spectra of syntan molecule, OCl^- and ClO_2.

The generation of $^*OCl$ and $^*OH$ during electrooxidation of syntan was also continuously monitored using electron spin resonance spectroscopy (ESR) coupled with spin

trapping technique.[25] Electron spin resonance spectroscopy (ESR) is used to identify free radicals. A free radical is a paramagnetic species containing an unpaired electron which exerts a magnetic moment that is detected by ESR. The free radicals are highly reactive with a life time of less than 20 s and hence their direct detection by ESR would be difficult to achieve. In order to overcome this difficulty, spin trap agents were used. The spin trapping agent reacts with a specific free radical to produce a more stable radical or spin adduct which is detected by ESR. In the presence of *OH radicals in the reaction mixture, the DMPO-OH adduct should yield a spectrum with characteristic intensity of 1:2:2:1. The ESR spectrum of DMPO-OCl adduct exhibit seven characteristic peaks (Fig. 4(a) and 4(b)).[25] In the present case, the ESR data confirm the generation of *OCl during electrooxidation of syntan. Though, the generation of *OH radicals during electrolysis was well established by previous researchers,[26,27] the absence of *OH radicals in this case may be explained due to co-generation of carbonate and bicarbonate ions which act as scavenging agents for hydroxyl radicals as shown in the following reactions.

In acidic pH

$$HCO_3^- + {}^{*}OH \longrightarrow CO_3^{-*} + H_2O \qquad (6)$$

Under alkaline pH

$$CO_3^{2-} + {}^{*}OH \longrightarrow CO_3^{-*} + OH^- \qquad (7)$$

Though the exact mechanism of the formation of carbonate radical is not fully established, it is known that the carbonate radical thus generated is further decayed to carbon dioxide

Therefore it is clear that the oxidation of phenolic syntan in the presence of NaCl is mediated predominantly by hypochloride ion and its free radical *OCl.

The low degradation of organics (70% of TOC) in the presence of $RuO_2/IrO_2/TiO_2$ coated titanium may be explained by the competition between the oxidation of organics and

the oxygen evolution reaction at the anode surface. The oxide coated electrodes have low over-potential for oxygen evaluation and hence the secondary reaction is favoured in comparison with oxidation of organic matter.[28] The oxidation of organics on noble oxide anode was attributed to the formation of "higher oxides" via adsorption of the hydroxyl / oxy chloride radical and its interaction with the oxygen already present in the oxide with a possible transition to higher oxide as mentioned below.

$$MOx + {}^{*}OH \longrightarrow MOx\,({}^{*}OH) \longrightarrow MO_{x+1} + H^{+} + e^{-} \quad (8)$$

$$MOx + {}^{*}OCl \longrightarrow MOx\,({}^{*}OCl) \longrightarrow MO_{x+1} + Cl^{-} \quad (9)$$

Since the solubility of chlorine in water is very high (6g/L) compared to oxygen (8 ppm), high concentration of oxidant with high oxidation reduction potential (ORP) would built up in the aqueous solution. Consequently even the refractory organics can be easily oxidized and degraded during electrooxidation. From the present study it is evident that oxidation of organics in the presence of chloride ion proceeds via adsorption of $^{*}OCl$ on metal oxide and the transition of oxygen atom to metal oxide, forming higher metal oxide as suggested in the above equation.

The cell voltage was found to decrease when the salt concentration was increased. This is due to increase in conductivity of the solution. The energy consumption (Fig. 5) was decreased from 8.06 kWh/kg of COD to 2.01kWh/kg of COD, when chloride concentration was increased from 1% w/v to 4% w/v. The inverse proportionality relationship between salt concentration and energy consumption may be attributed to increase in active chloro species and decrease in cell voltage when the salt concentration was increased. General current efficiency was found to increase with increase in NaCl concentration due to the formation of chlorine and hypochlorous acid/hypochlorite ion in very high concentrations.

The influence of current density on degradation was also studied by varying the current density from 0.005 A/cm^2 to 0.0025 A/cm^2. The NaCl concentration and the initial pH was maintained at 3% at 10.0 respectively. From results it is evident that the degradation rate was increased with increase in current density (Fig. 2). It could be attributed the formation of more oxidizing agents. There was no significant change in COD beyond 0.020 A/cm^2.

Energy consumption (EC) and General Current Efficiency (GCE)

Further the energy consumption (EC) and general current efficiency (GCE) were also calculated using the following equations and the results are given as in Fig. 5.

Total Current Efficiency (TCE)

$$TCE = \frac{\left[COD_t - COD_{t+\Delta t}\right]}{8I\Delta t} \qquad (10)$$

Where COD_t and $COD_{t+\Delta t}$ are chemical oxygen demands in gram of O_2 per dm^3 at times t and t+Δt respectively; F is Faraday constant (96487 C mol^{-1}); V is the volume of electrolyte in litre and I is the current in Ampere and 8 is the equivalent mass of oxygen (g/eq^{-1}).

Energy consumption for the removal of one Kg of COD was calculated. It is expressed in kWh.kg^{-1} of COD or TOC.

$$Energy\ consumption = \frac{\left[tVA/S_v\right] \Big/ 1\times10^3}{\Delta COD \Big/ 1\times10^6}\ Kwh/kgCOD \qquad (11)$$

Where, t is the time of electrolysis in hours, V is the average cell voltage, A is Ampere, S_V is sample volume in litres and ΔCOD is the difference in COD in time t in mg/L.

The current efficiency was found to decrease when the current density was increased. This may be explained due to higher rate of oxygen evolution compared to oxidation of organics at the anode surface. In general, if the applied current is more than the limiting current, the oxidation will be invariably under mass transport control and the oxygen evolution dominates the oxidation.

Fourier Transform - Infrared Spectroscopy (FT-IR) study

The FT-IR spectra of the syntan and the sample resulting from the electrooxidation (obtained by lyophilisation) was recorded and shown in Fig.6. The broad absorption band around 3350 cm^{-1} observed in the FT-IR spectrum of phenolic syntan could be assigned to -OH stretching vibrations. The peak with medium intensity at 1568 cm^{-1} may be assigned to C=C stretching vibrations and the high intensity peak at 1116 cm^{-1} could be attributed to –C=O stretching vibrations. The sharp peak with medium intensity around 1035 cm^{-1} may be assigned to S=O stretching vibrations of SO_3H attached to phenol ring. The broad peak around 3435 cm^{-1} observed in the spectrum of oxidized syntan sample could be assigned to O-H stretching vibrations. The sharp peak with high intensity at 1635 cm^{-1} is a characteristic *ν*(C=O) vibration of quinone functional group. The peak with medium intensity at 1391 cm^{-1} may be assigned to C-O-H bending. The low intensity peak at 996 cm-1 could be assigned to COOH bending vibrations. Thus the FT-IR spectrum of the electrooxidation sample clearly indicates the presence of carboxylic acids. It is apparent that the polymer is ultimately mineralized to CO_2 and H_2O via low molecular weight carboxylic acids like formic acid and oxalic acid. The presence of these acids in oxidized sample was established by NMR spectroscopy.

Nuclear Magnetic Resonance (NMR) study

In order to have better clarity on the oxidation of syntan during electrooxidation, NMR spectrum was taken to identify the compounds formed during oxidation. Fig. 7(a) shows the ^{13}C-CP/TOSS spectrum of phenolic syntan run in solid state at room temperature. It shows characteristics peaks arising from the constituents of phenolic syntan. The peak with moderate intensity at 40 ppm is assigned to methylene bridge of phenolic syntan. Six peaks are seen with varying intensity in the range of 115-161 ppm The chemical shift value and their assignment are shown in Table 1. The presence of two peaks at 160.4 and 156.55 ppm is attributed to carbons to which OH functionality is attached. The phenyl ring carbons show peaks in the range of 115-140 ppm. The individual assignment ring carbons are arrived by comparing the literature data are listed in Table 1. These features are consistent with the structure of phenolic syntan as shown in Fig.7(a).

Fig. 7(b) shows the ^{13}C-CP/TOSSNMR of oxidized sample of phenolic syntan during electro-oxidation. Remarkably, the spectrum shows only one intense peak at 164.35 ppm with few shoulders. In contrast to phenolic resin where more than six peaks are seen the appearance of one peak for the electro-oxidized (120 min) phenolic syntan clearly suggests that the aromatic moieties are broken. The high intense peak seen at 164.35 ppm of electro-oxidaized phenolic syntan is attributed to formic acid/oxalic acid residual moiety. This is based on the fact that the carbonyl region of the acid is 160-165 ppm. Further, the disappearance of peaks arising from phenyl ring and methylene bridge supports oxidation of the phenolic syntan leading to the formation of oxalic acid and formic acid.

Adsorbable Organic Halogens (AOX)

The samples collected at different time intervals of electrooxidation was analysed for the presence of chloro-organic compounds. The results of AOX analysis have revealed the

absence of chloro-organics at any point of time during electro-oxidation. The results demonstrate that the electrooxidation is a cleaner and promising process compared to other processes.

Kinetics of degradation

In indirect electrochemical treatment, degradation of organic compound is predominantly due to electrically generated chlorine/hypochlorite. Therefore, COD removal rate is directly proportional to the concentration of organic compound (phenolic syntan) and the chlorine/hypochlorite. The data of ln C/C_0 was fitted for zero order, first order and second order equations. The equations for the orders zero, first and second are y=-0.2098x+1.08, y=-0.5025x+0.4633 and y=1.5962x+1.1956 with R^2 values 0.878, 0.996 and 0.943 respectively. The best fit (R^2) was obtained for first order reaction. The first order rate constant calculated from the slope of the plot is 16.70 x 10^{-3} min (Fig. 8). Therefore it could be concluded that the process of electrolytic degradation is dependent solely on the concentration of phenolic resin.

Degradation pathway

The possible degradation pathway of electro-oxidation of phenolic syntan is shown in figure (Fig. 9). Initially, the polymer is degraded to hydroquinone and benzoqunone during electrooxidation. Breakdown of quinone compound as progresses is also evident from FT-IR and NMR spectra. The polymeric syntan is finally degraded to formic acid before converting to CO_2.

Study on passivation of electrodes by Scanning Electron Microscope/Energy Dispersive Sperctroscopy (SEM/EDAX)

The problem of passivation of electrodes and the formation of polymeric films on the electrodes during electro-oxidation of phenolics was reported.[29] Blocking polycrystalline platinum Pt and boron-doped diamond BDD electrodes by 20 phenolic compounds was studied by means of chronoamperometric and theoretical methods.[30] The polymerization process was studied as a function of the methyl substitution in the phenolic structure. Electrochemical quartz crystal microbalance studies show that the polymer formed from substituted phenols is more passivating than that from the non-substituted phenol. In any case, the largest amount of mass was deposited during the first voltammetric cycle and the Pt electrode was more active than the Au electrode for the organic electrooxidation process.[30] The process of passivation is governed by many factors such as electrode material, current density, type of phenolic compound and electrolyte concentration. Therefore studies to verify the possible passivation is equally essential while evaluation the oxidation process. The electrode surface was investigated using scanning electron microscope with EDAX facility. The micrographs shown in Fig.10, indicated that there was no coating or passivation on the electrode surface. Major elements detected by EDAX and the composition of the electrodes were presented in Table 2. It is evident that atomic weight % of the elements present in the electrodes is more or less same even after the electro-oxidation of phenolic syntan. Thus it is evident that there is no change in the electrode composition due to deposition of organic matter during electrolysis. It is also evident that there is no passivation of electrodes due to deposition of syntan polymer on the electrode surface.

Conclusions

The Degradation of recalcitrant phenolic syntan by electrooxidation was investigated using $RuO_2/IrO_2/TiO_2$ coated titanium electrodes. The generation of oxidants such as Cl_2, HOCl and free radicals of oxychloride were found to play a major role in the oxidation of organics. The generation of $^{*}ClO$ free radical was ascertained using electron spin resonance (ESR) spectroscopy coupled with spin trapping technique. The intermediate compounds formed during electrooxidation were characterised using AOX, FT-IR and NMR techniques and the possible degradation pathway was suggested. The polymeric syntan was initially converted to benzoquinone which inturn is oxidized to low molecular weight compounds such as oxalic and formic acids. It was observed that the oxidation of phenolic syntan was proportional to the current density and electrolyte concentration. The kinetics of the degradation of phenolic syntan was found to follow first order rate equation with an R^2 value of 0.9966. It was also observed that chloroorganic compounds were not formed during electro-oxidation of phenolic syntan. Further it was found that there was no passivation of electrodes.

Experimental

Materials

The phenolic syntan (phenolic polymer) viz., Basyntan DI was obtained from M/s BASF India Ltd., Chennai, India. The syntan was quantitatively analysed for C, H, N, and S and found to be 32.24%, 3.25%, 1.81% and 11.90% respectively. The characteristic UV-Visible absorbance (λ_{max}) was noticed around 280 nm. The other chemicals used were of analytical grade and procured from M/s Sigma-Aldrich, India.

Electro-oxidation setup

The schematic diagram of experimental setup is shown in Fig.1. Reactor with a working volume of 2.0 litres was fitted with titanium electrodes coated with $TiO_2/RuO_2/IrO_2$. The working surface area of the electrode was estimated to be 380 cm^2. Both the anode and cathode were placed vertically and parallel to each other with a gap of 1.0 cm between anode and cathode to minimize the omhic loses. A D.C regulated current ranging from 0 to 25A was used. A peristaltic pump was used for circulating the syntan solution under constant flow of 300 mL/min.

The phenolic polymer (Basyntan DI) solution with a concentration of 1000 mg/L was prepared using distilled water. Required quantity of NaCl was added and the pH was adjusted using dilute HCl and NaOH solutions.

Analysis

The degradation of syntan was followed by measuring the total organic carbon (TOC) / and chemical oxygen demand (COD). During the experiment, samples were drawn at different intervals and analysed. TOC was determined using ELEMENTER - Vario TOC Select analyzer. The COD was determined by the standard procedure reported by American public health association.[31] In order to eliminate the interference of chloride ion, mercuric sulphate was added in the COD estimation. Elements present in phenolic polymer were analyzed by Elemental analyzer (Model: Vario Micro Cube; Make: M/s Elementer, Japan). The pH of the solution was measured using pH meter (HACH model HQ40d). The UV-Vis spectrophotometer (JASCO-V600) and FT-IR (JASCO-4200) were used to follow the degradation of syntan during electrooxidation. All the results reported are the arithmetic mean of three samples.

Characterization of free radicals

Electron Spin Resonance (ESR) spectrometry coupled with spin trapping technique was employed to identify the free radicals generated during electro-oxidation. 5,5,-dimethyl-1-pyrroline-N-oxide (DMPO) was used as spin trapping agent. Prior to using, the DMPO was purified using activated charcoal to avert the free radicals. ESR spectra were recorded using BRUKER spectrometer operating at the X band and flat cell assembly. For each sample six scans were recorded at a modular frequency of 10 kHz. Data acquisition and instrument control were performed by Bruker software. All the experiments were carried out at room temperature and ambient air.

NMR study

NMR analysis was carried out in 400MHz Bruker WB Avance III NMR spectrometer ^{13}C frequency = 100 MHz) and 4 mm probe head were used. The NMR spectrum was recorded using Zgpg 30 pulse sequence. Processing and plotting was done using Top Spin NMR software.

Acknlowdgement

The authors wish to thank Dr. Narasimha Swamy, Polymer division of CLRI for his valuable suggestions on spectroscopic studies. The financial support of CSIR-HRDG and CSIR-CLRI project ZERIS (CSC 0103) is acknowledged. This work forms a part of the doctoral program of the first author who is Senior Research Fellow at CSIR-NML.

References

1. J. R. Rao, N. K. Chandrababu, C. Muralidharan, B. U. Nair, P. G. Rao and T. Ramasami, *Journal of Cleaner Production*, 2003, **11**, 591-599.

2. P. M. de Aquim, M. Gutterres and J. Trierweiler, *Journal of the Society of Leather Technologists and Chemists*, 2010, **94**, 253-258.

3. J. Michalowicz and W. Duda, *Polish Journal of Environmental Studies*, 2007, **16**, 347-362.

4. A. Ginos, T. Manios and D. Mantzavinos, *Journal of Hazardous Materials*, 2006, **133**, 135-142.

5. S. Thomas, S. Sarfaraz, L. C. Mishra and L. Iyengar, *World Journal of Microbiology & Biotechnology*, 2002, **18**, 57-63.

6. P. J. Welz, J. B. Ramond, D. A. Cowan and S. G. Burton, *Bioresource Technology*, 2012, **119**, 262-269.

7. V. C. Srivastava, M. M. Swamy, I. D. Mall, B. Prasad and I. M. Mishra, *Colloids and Surfaces a-Physicochemical and Engineering Aspects*, 2006, **272**, 89-104.

8. A. Demirev, *Oxidation Communications*, 2008, **31**, 812-818.

9. L. N. Kruthika, G. B. Raju, and S. Prabhakar, *Material Science Forum,* 2013, 734, 117-126.

10. F. Ferella, I. De Michelis, C. Zerbini and F. Veglio, *Desalination*, 2013, **313**, 1-11.

11. S. Sundarapandiyan, R. Chandrasekar, B. Ramanaiah, S. Krishnan and P. Saravanan, *Journal of Hazardous Materials*, 2010, **180**, 197-203.

12. K. S. Min, J. J. Yu, Y. J. Kim and Z. Yun, *Journal of Environmental Science and Health Part a-Toxic/Hazardous Substances & Environmental Engineering*, 2004, **39**, 1867-1879.

13. G. B. Raju, M. T. Karuppiah, S. S. Latha, S. Parvathy and S. Prabhakar, *Chemical Engineering Journal*, 2008, **144**, 51-58.

14. M. G. Tavares, L. V. A. da Silva, A. M. Sales Solano, J. Tonholo, C. A. Martinez-Huitle and C. L. P. S. Zanta, *Chemical Engineering Journal*, 2012, **204**, 141-150.

15. M. Gotsi, N. Kalogerakis, E. Psillakis, P. Samaras and D. Mantzavinos, *Water Research*, 2005, **39**, 4177-4187.

16. G. A. Ciorba, C. Radovan, I. Vlaicu and S. Masu, *Journal of Applied Electrochemistry*, 2002, **32**, 561-567.

17. J.-H. Yoon, J. Yang, Y.-B. Shim and M.-S. Won, *Bulletin of the Korean Chemical Society*, 2007, **28**, 403-407.

18. P. Canizares, J. Garcia-Gomez, C. Saez and M. A. Rodrigo, *Journal of Applied Electrochemistry*, 2004, **34**, 87-94.

19. M. Panizza, C. Bocca and G. Cerisola, *Water Research*, 2000, **34**, 2601-2605.

20. M. Li, C. Feng, W. Hu, Z. Zhang and N. Sugiura, *Journal of Hazardous Materials*, 2009, **162**, 455-462.

21. H. Ma, X. Zhang, Q. Ma and B. Wang, *Journal of Hazardous Materials*, 2009, **165**, 475-480.

22. C. Belaid, M. Khadraoui, S. Mseddi, M. Kallel, B. Elleuch and J. F. Fauvarque, *Journal of Environmental Sciences-China*, 2013, **25**, 220-230.

23. K. B. Divya, Keerthi and N. Balasubramanian, *Research Journal of Chemistry and Environment*, 2013, **17**, 19-24.

24. T. Rema and R. A. Ramanujan, Journal of Scientific & Industrial Research, 2012, **71**, 363-368.

25. Silvia D. Stan, (2003) Bacterial inhibition by electrolyzed oxidizing water and application to disinfection of sprout seeds. Thesis submitted for the degree of Doctor of Philosophy in Food Science and Technology, Oregon State University.

26. M. Panizza and G. Cerisola, *Environmental Science & Technology*, 2004, **38**, 5470-5475.

27. M. Panizza and G. Cerisola, *Chemical Reviews*, 2009, **109**, 6541-6569.

28. C. Comninellis, *Electrochimica Acta*, 1994, **39**, 1857-1862.

29. M. Ferreira, H. Varela, R. M. Torresi and G. Tremiliosi-Filho, *Electrochimica Acta*, 2006, **52**, 434-442.

30. R. F. Teofilo, R. Kiralj, H. J. Ceragioli, A. C. Peterlevitz, V. Baranauskas, L. T. Kubota and M. M. C. Ferreira, *Journal of the Electrochemical Society*, 2008, **155**, D640-D650.

31. APHA. 1995. Standard methods. 19th Edition. American Public Health Association, Washington, DC.

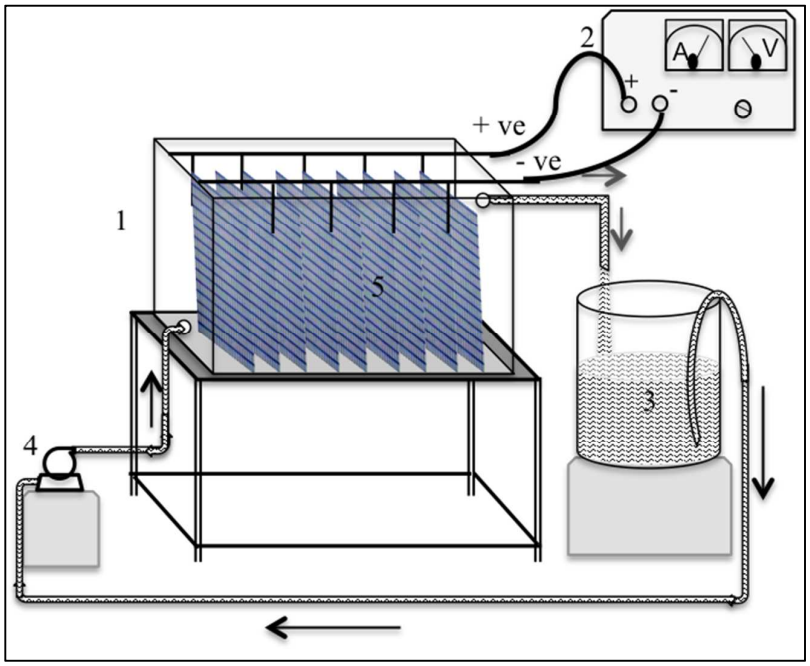

Fig. 1 Schematic diagram of electro-oxidation setup: 1. Electro-oxidation Tank; 2. DC power source; 3. Phenolic syntan solution; 4. Peristaltic pump; 5. Anodes and cathodes

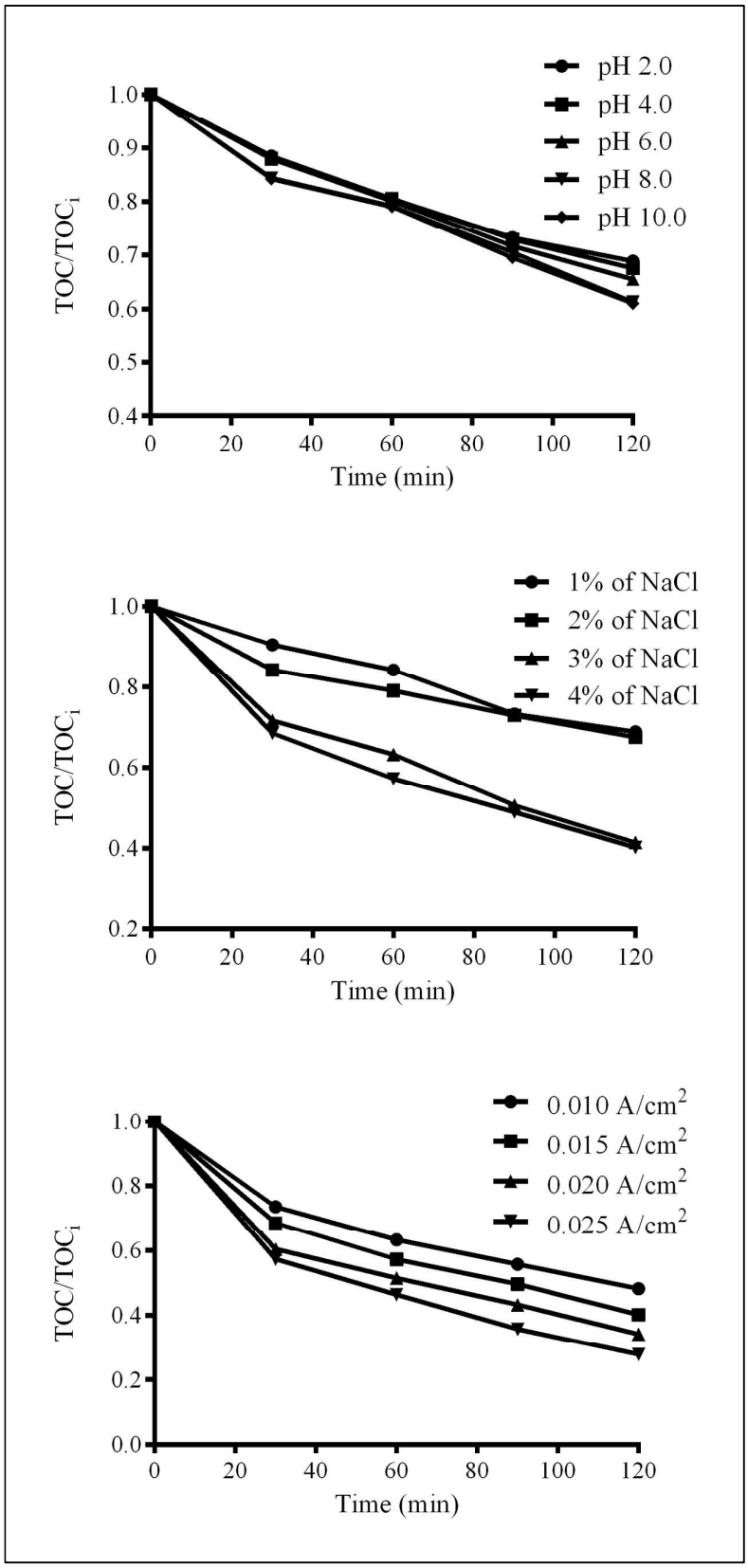

Fig. 2 Effect of operational parameters (a) pH, (b) Electrolyte concentration (c) Current density on COD and TOC reduction rate with electrolysis time

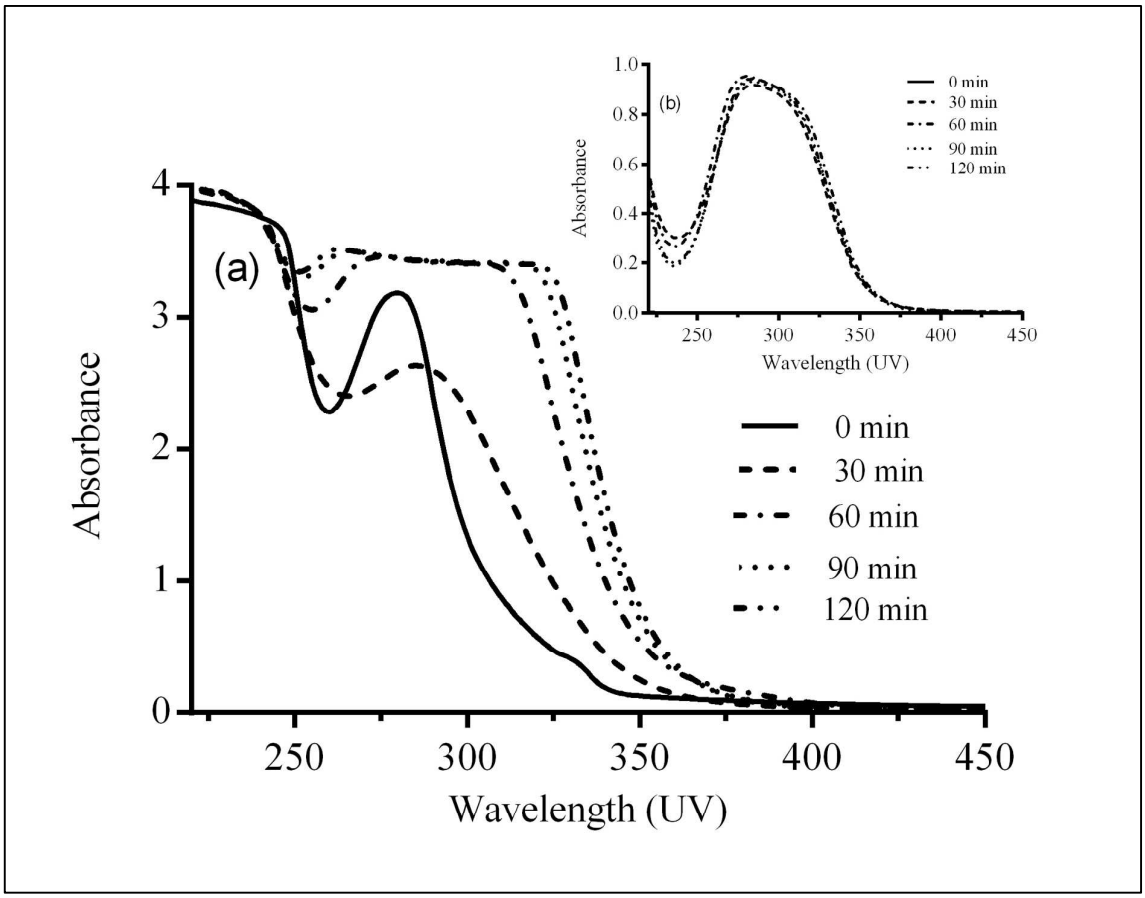

Fig. 3 UV-Vis spectrum for electro-oxidation of (a) phenolic resin and (b) in the absence of phenolic syntan at different time of electro-oxidation (Current density 0.015 A/cm^2 , pH 9.0, concentration of electrolyte 3.0% and duration of electrolysis: 120 min).

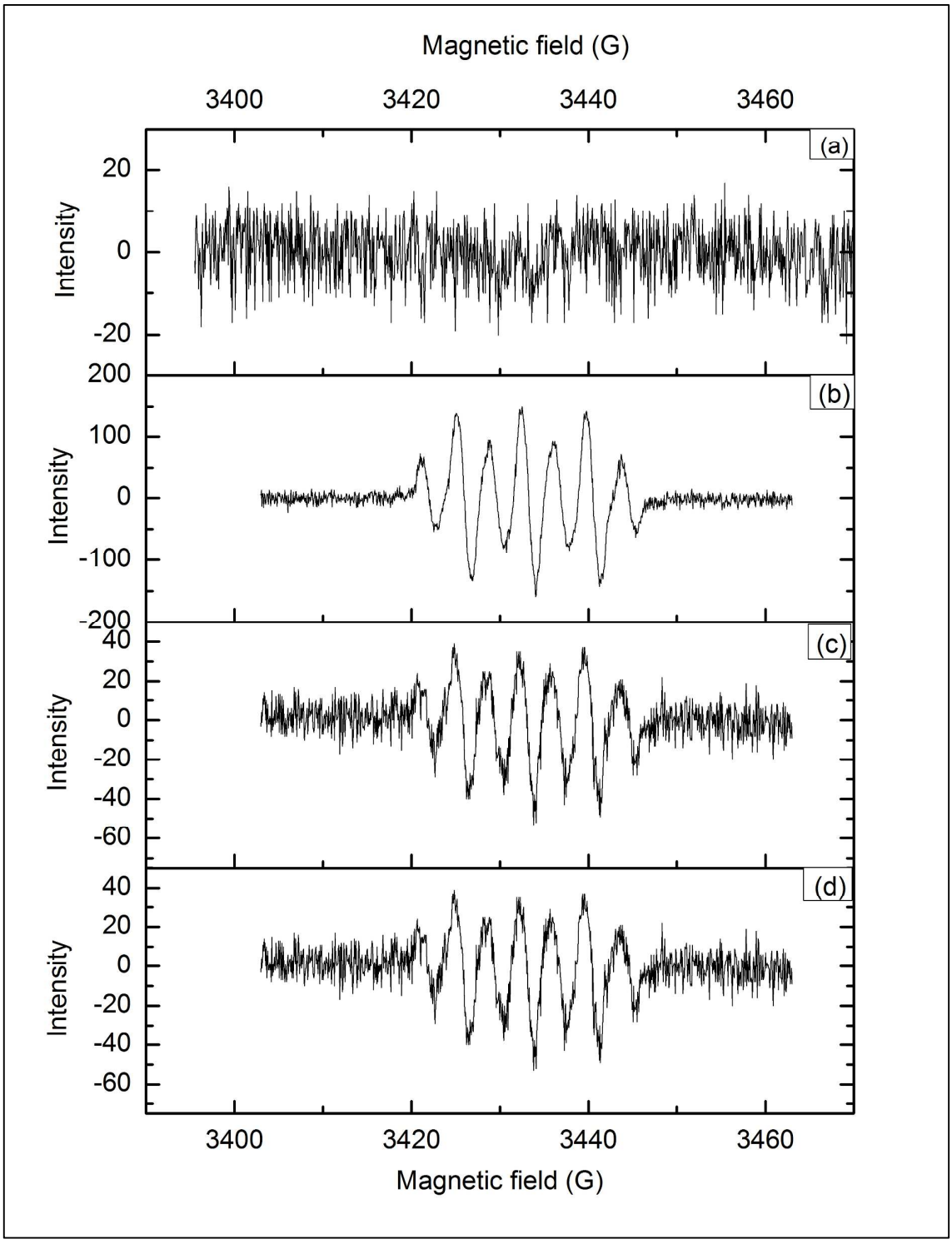

Fig. 4(a) ESR spectra of phenolic syntan samples collected at different time intervals of electro-oxidation (a) 0 min, (b) 10 min, (c) 20 min and (d) 30 min. (Current density 0.015 A/cm^2, pH 9.0 and concentration of electrolyte 3.0%).

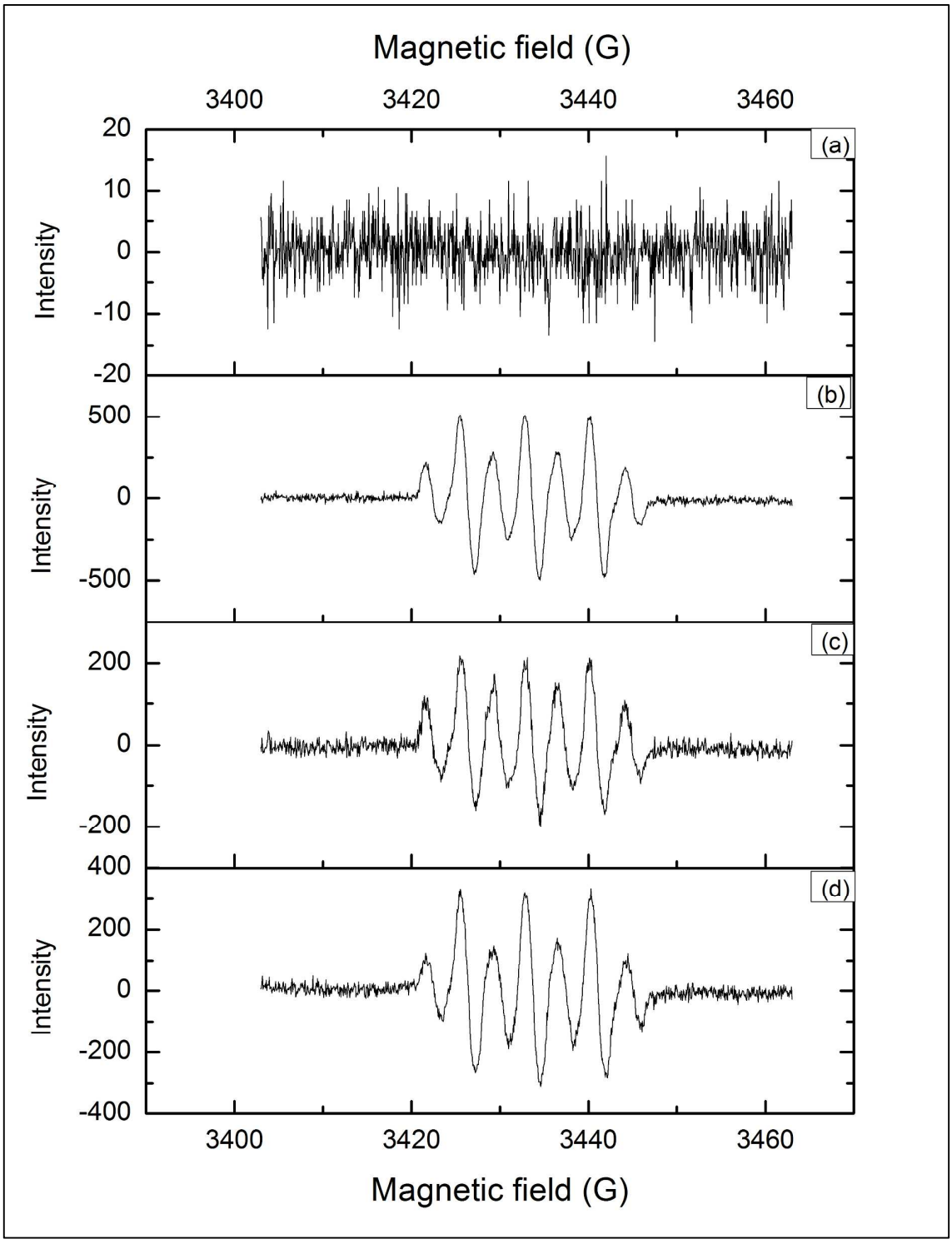

Fig. 4(b) ESR spectra of samples collected during electrolysis of NaCl in the absence of phenolic syntan at (a) 0 min, (b) 10 min, (c) 20 min and (d) 30 min. (Current density 0.015 A/cm^2, pH 9.0 and concentration of electrolyte 3.0%).

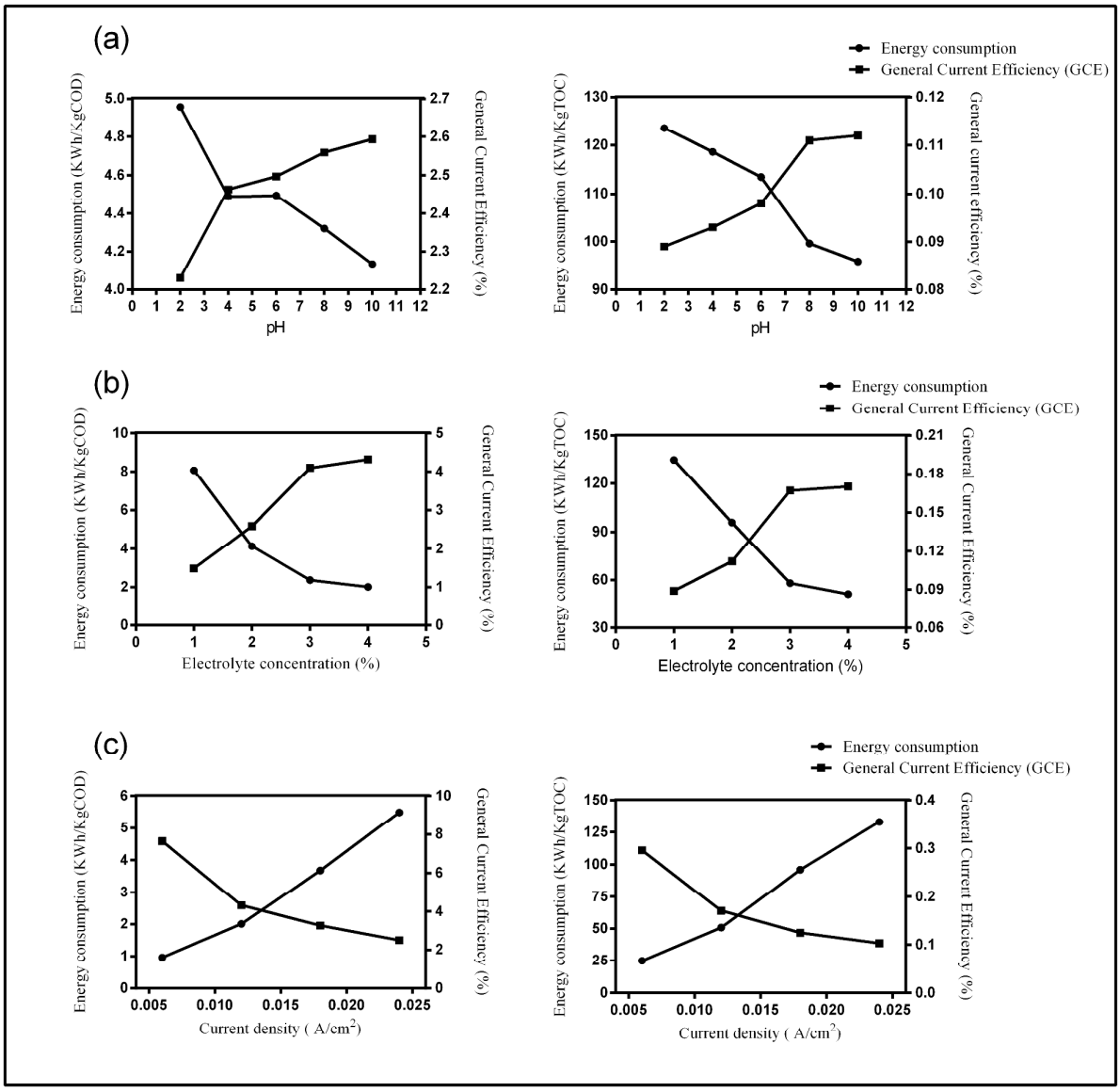

Fig. 5 Comparison of energy consumption and General Current Efficiency at various conditions of electro-oxidation (a) pH; (b) Electrolyte Concentration; (c) Current density; (Electrolysis time: 120 min).

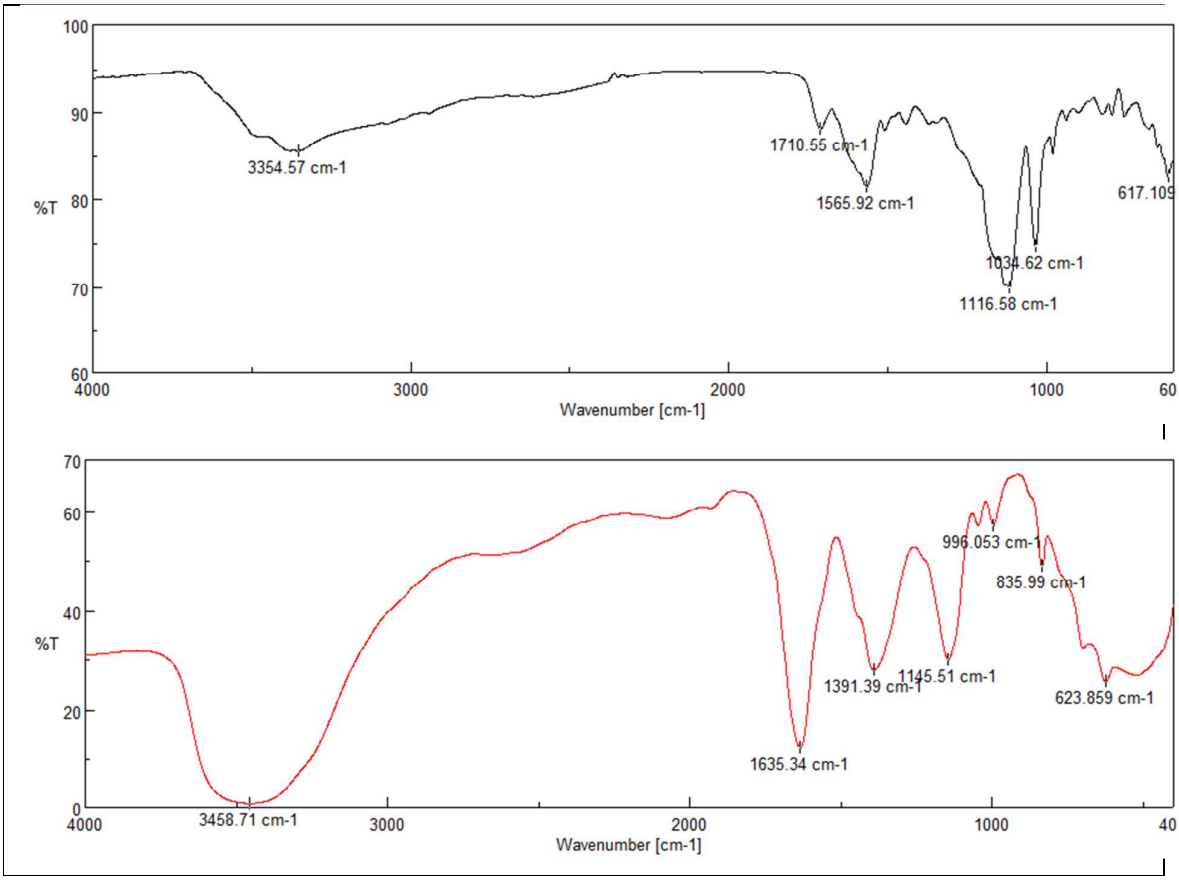

Fig. 6 FT-IR spectrum of phenolic syntan, (a) before electro-oxidation and (b) at the 120 min of electro-oxidation (Current density 0.015 A/cm^2, pH 9.0, concentration of electrolyte 3.0% and electrolysis time 120 min).

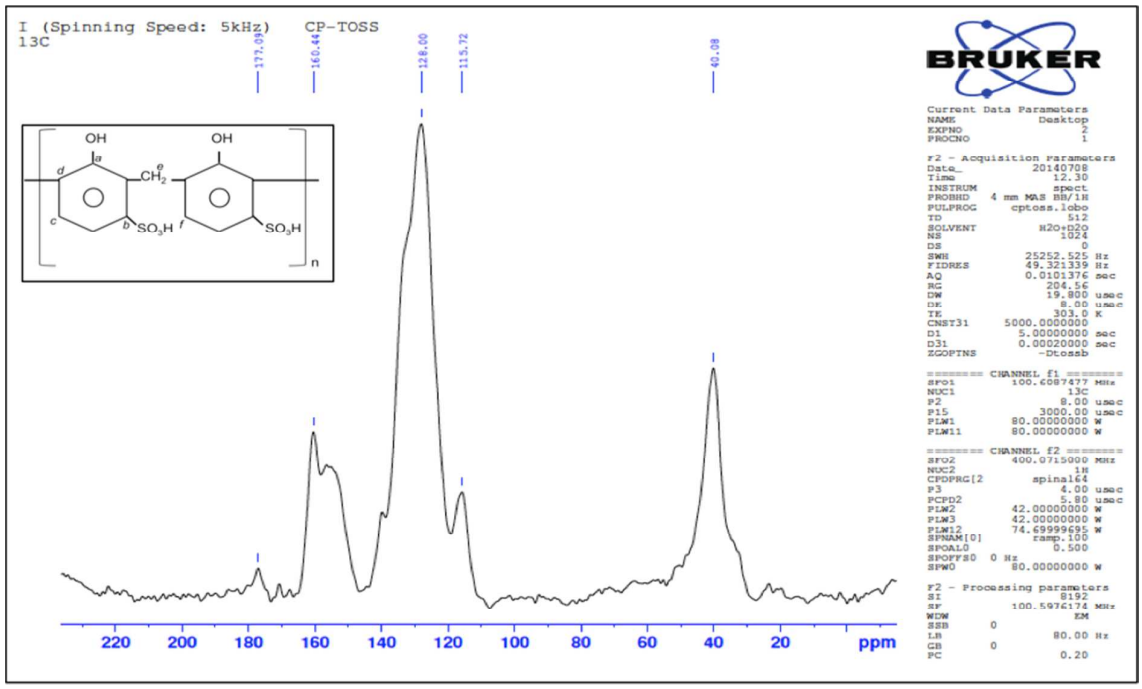

Fig. 7(a) ^{13}C-CP/TOSS spectrum of phenolic syntan before electrochemical degradation

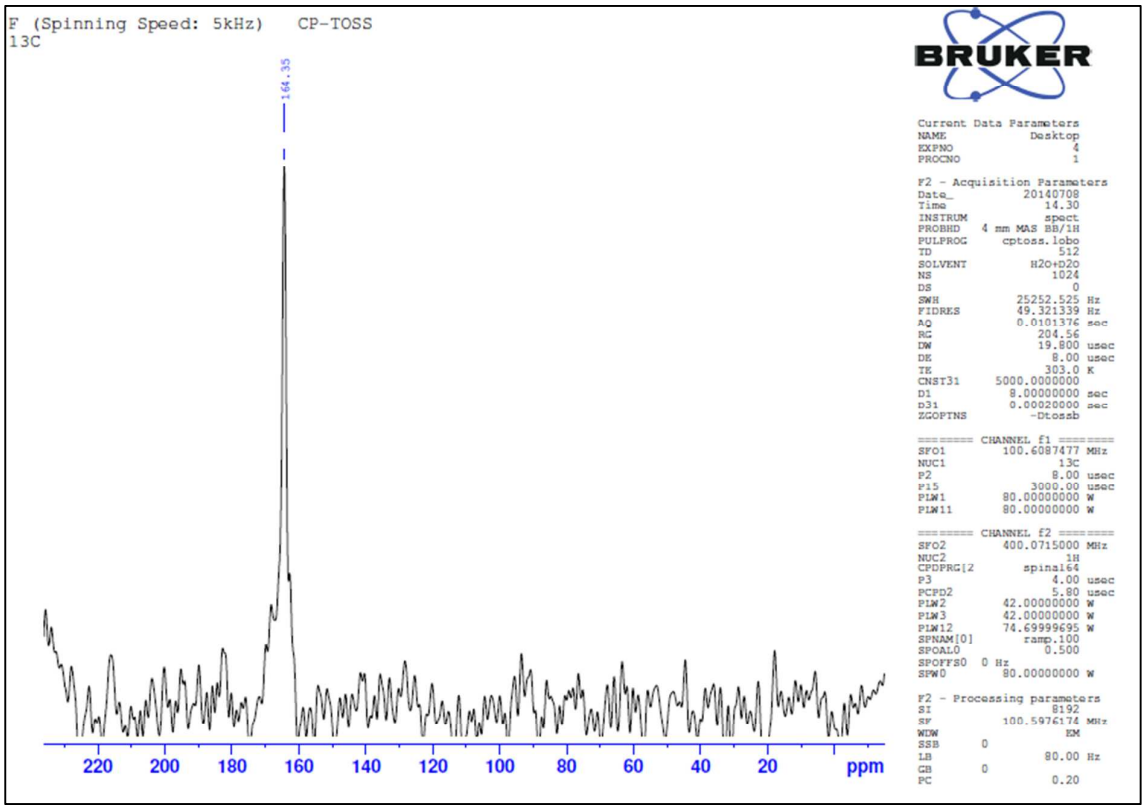

Fig. 7(b) ^{13}C-CP/TOSS spectrum of phenolic syntan after electrochemical degradation (Current density 0.015 A/cm^2 , pH 9.0, concentration of electrolyte 3.0% and duration 120 min).

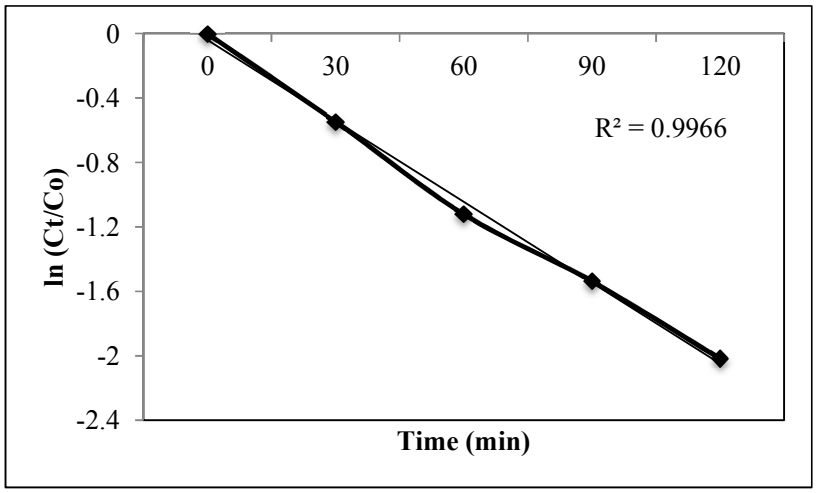

Fig. 8 Kinetics for electrochemical degradation of phenolic syntan (A=0.015A/cm^2); Electrolyte concentration = 3%; pH = 9.0 and time = 120 min)

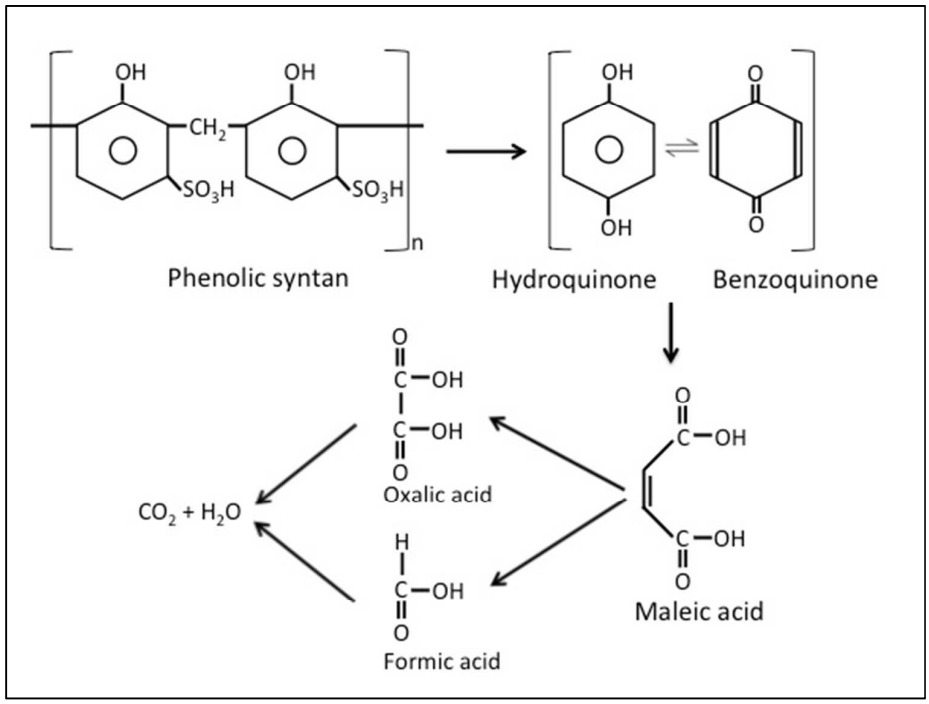

Fig. 9 Possible degradation pathway of phenolic syntan during electrochemical degradation

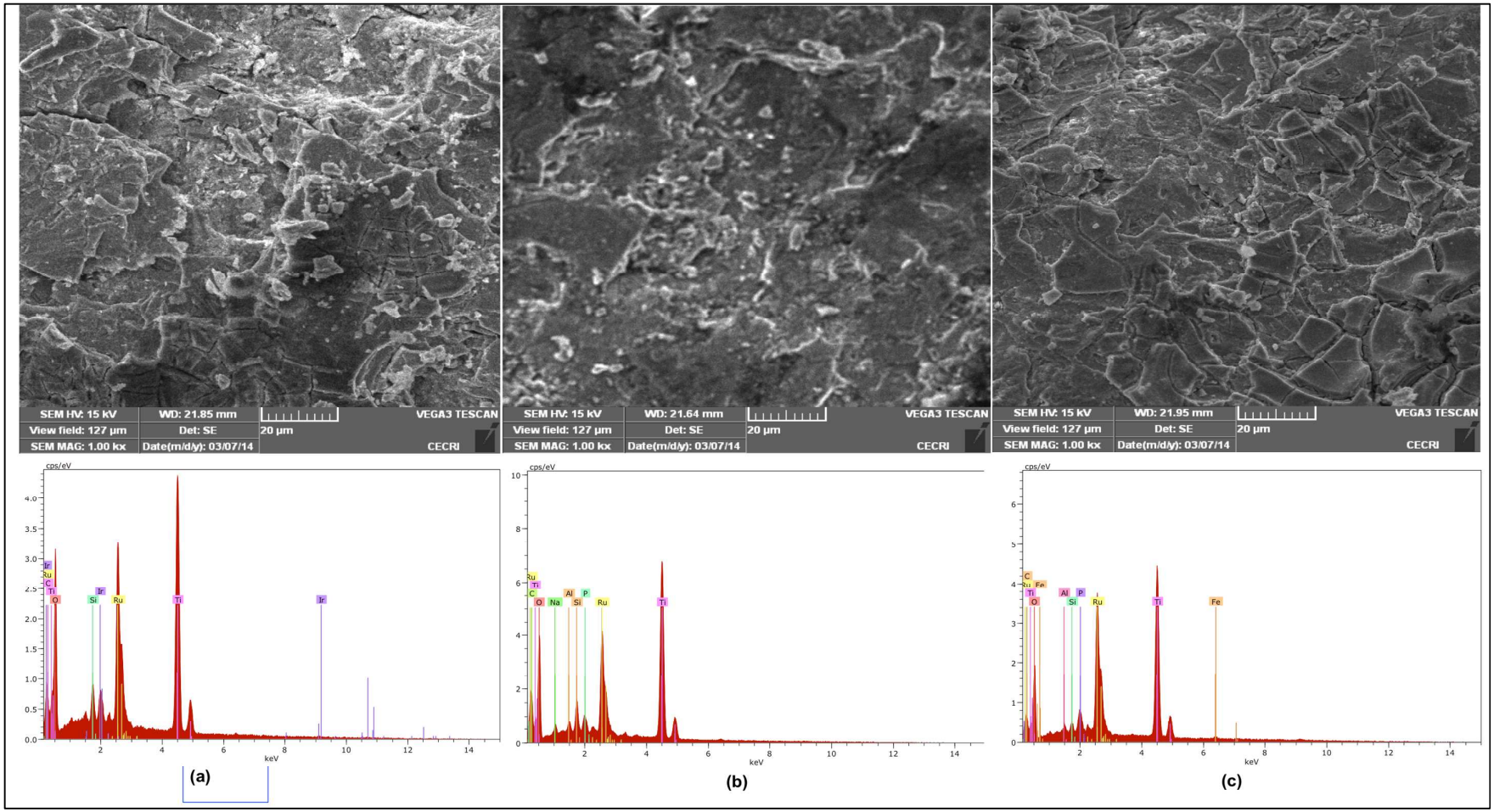

Fig. 10 SEM-EDAX micrographs and spectra presenting the chemical composition of the electrodes surface of (a) Before oxidation, (b) After oxidation: Anode and (c) After oxidation: Cathode

Table 1. Chemical shift values ^{13}C NMR of phenolic syntan (Before and after electrochemical degradation)

Assignment	Chemical shift (ppm)	Assignments of carbons
a	156.55	Phenoxy region
b	139.70	C-SO_3H
c	131.90	Meta, substituted *ortho*, substituted *para*
d	115.70	Unsubstituted ortho position
e	40.80	Para-para methylene bridges
f	128.00	Meta, substituted *ortho*, substituted *para*

Table 2. Elemental composition (weight % and Atomic Weight %) of electrodes surfaces from EDAX spectrum

Elements	Before Electro-oxidation		After Electro-oxidation			
			Cathode		Anode	
	Weight (%)	Atomic weight (%)	Weight (%)	Atomic weight (%)	Weight (%)	Atomic weight (%)
Ti	31.50	21.97	28.92	27.12	32.22	21.26
O	31.20	65.10	29.28	57.62	29.65	58.55
Ru	16.45	5.44	17.57	7.80	13.90	4.34
C	1.91	5.30	1.52	2.17	4.81	12.64
Si	0.99	1.18	ND	ND	1.23	1.38
P	0.95	1.02	0.78	1.13	0.73	0.75